PCCP

PAPER

View Article Online
View Journal | View Issue



Cite this: *Phys. Chem. Chem. Phys.*, 2026, **28**, 751

# Isotopic chirality and high-resolution gigahertz and terahertz spectroscopy of *trans*-2,3-dideutero-oxirane (*tc*-CHDCHDO)

Ziqiu Chen, *[ab] Sieghard Albert, [b] Karen Keppler, [b] Gunther Wichmann, [b] Martin Quack, *[b] Volker Schurig[c] and Oliver Trapp [d]

Received 15th August 2025,
Accepted 4th November 2025

DOI: 10.1039/d5cp03143e

rsc.li/pccp

We report the observation and assignment of the rotational spectra of the isotopically chiral molecule, *trans*-2,3-dideutero-oxirane (*tc*-CHDCHDO) measured with the Zurich gigahertz (GHz) spectrometer (64 to 500 GHz and $\Delta\nu/\nu = 10^{-11}$) and with our highest resolution Fourier transform infrared spectrometer at the Swiss synchrotron light source (SLS) (best instrumental resolution $\Delta\tilde{\nu} = 0.00053$ cm$^{-1}$) in the terahertz range (far infrared from 25 to 80 cm$^{-1}$). The combined GHz and THz spectra were analysed using an accurate effective Hamiltonian providing newly determined rotational parameters, which are crucial for the prediction of *trans*-2,3-dideutero-oxirane transitions to be observed by astrophysical spectroscopy. The recent detection of singly deuterated oxirane in the protostar IRAS 16 293–2422 B based on our previous predictions highlights the potential for the detection of doubly deuterated oxiranes including *trans*-2,3-dideutero-oxirane. These offer insights into deuterium fractionation in space and the formation mechanisms of complex and in particular chiral molecules. This study is also related to the new isotope effect in isotopically chiral molecules characterised by the parity violation energy differences of the ground states of the enantiomers and to biomolecular homochirality. In addition, we report the analysis of the pure rotational spectra of *cis*-2,3-dideutero-oxirane also present in our experimental spectra in the GHz range.



## 1. Introduction

Chiral symmetry breaking[1] in molecules that are chiral only by isotopic substitution results in several important effects ranging from quantum structure to anharmonic vibrational quantum dynamics and finally parity violation, which introduces a fundamentally new isotope effect.[2–10] Indeed, in such ''isotopically chiral molecules'', a small parity violating energy difference $\Delta_{pv}E$ between the ground states of the enantiomers is predicted, which arises through the weak nuclear interaction from the different weak nuclear charge of the isotopes with different numbers of neutrons.[2–7] While calculated to be very small, on the order of feV to aeV depending on the molecule, this could, in principle, be measured in special experiments,[2,11,12] although until now no successful experiment has been reported (see the reviews in ref. 9 and 10). On the other hand, when neglecting the parity violating weak nuclear force, which is the common assumption in current quantum chemical theory, $\Delta_{pv}E$ would be exactly zero by symmetry.

A further interesting aspect of isotopically chiral molecules is related to astrophysical spectroscopy: the detection of an achiral ''parent molecule'' can lead to the detection of a corresponding isotopically chiral molecule. In this context we have initiated some time ago a spectroscopic project on isotopically chiral oxirane derivatives, given the well-established astrophysical detection of the achiral oxirane molecule (ethylene epoxide, *cyclo*-$C_2H_4O$).[13–18] Starting with high resolution GHz and THz (FTIR) spectroscopy of monodeutero-oxirane,[19] our prediction of some relevant spectral lines in the range 300 to 400 GHz led, indeed, to the astrophysical detection of this molecule in IRAS 16293-2422B using ALMA (the Atacama Large Millimetre/submillimetre Array),[20] see also ref. 21 for further spectroscopic results.

Chiral molecules are of particular astrophysical interest, because the detection of some systematic extraterrestrial homochirality would be a very strong indication for extraterrestrial life, as there is no known chemical mechanism except the biochemistry of life which would generate a consistent global homochirality.[22,23] While various techniques for analysis are possible by sending missions within the solar system,[24] only a

[a] *College of Chemistry and Chemical Engineering, Lanzhou University, Lanzhou 730000, China. E-mail: chenziqiu@lzu.edu.cn*
[b] *Department of Chemistry and Applied Biosciences, ETH Zurich, CH-8093 Zurich, Switzerland. E-mail: martin@quack.ch*
[c] *Institute of Organic Chemistry, University of Tübingen, Tübingen, Germany*
[d] *Department of Chemistry, Ludwig-Maximilians-University, Munich, Germany*

spectroscopic approach (using circular dichroism or high resolution vibrational circular dichroism, for instance[22,23]) would be able to go beyond the solar system, say, by the spectroscopy of exoplanetary atmospheres.[25–27] While chirally sensitive astrophysical spectroscopy in this context is not to be expected in the nearest future, the spectroscopic detection of chiral molecules beyond the solar system prepares a path for such future studies. So far, only two chiral molecules have been detected by astrophysical spectroscopy in the interstellar medium (ISM), monodeutero-oxirane as already mentioned[19–21] and methyloxirane.[28] Clearly more effort is needed towards identifying further chiral molecules for such observations.

In the present publication we report our results on the isotopically chiral *trans*-2,3-dideutero-oxirane as a further chiral oxirane isotopomer likely to be observed in a way analogous to monodeutero-oxirane. *Trans*-2,3-dideutero-oxirane (or *trans*-[2,3-$^2H_2$] oxirane, *trans-cyclo*-CHDCHDO, short-hand used here as *tc*-CHDCHDO, see Fig. 1) has been a prototypical chiral compound for experimental and theoretical studies of vibrational circular dichroism for some time,[29–38] and it has also been used more recently as an example for the direct determination of absolute configuration by Coulomb explosion imaging (CEI)[39–42] (see also ref. 43 for an alternative technique used for the chiral prototype molecule CHFClBr[43] as compared to the "classic" approach using X-ray crystallography[44,45]). However, so far only very little high resolution spectroscopic work exists for *tc*-CHDCHDO. Indeed, there seems to be only the singular early microwave spectroscopy of the various oxirane isotopomers by Hirose,[46,47] which reported 21 rotational transitions for *tc*-CHDCHDO with the overall aim of a structure determination from the rotational constants of several isotopomers. Here, we shall report the first extensive study of rotational transitions in the GHz range (64 to 500 GHz) and the THz range by synchrotron-based Fourier transform infrared (FTIR) spectroscopy (0.75 to 2.4 THz), thus covering most of the rotational spectrum with a remaining gap only from 500 to 750 GHz. The analyses of more than 4000 assigned line positions provide accurate rotational parameters for the vibrational ground state and a very accurate basis for the prediction of lines for the astrophysical detection of *tc*-CHDCHDO among other possible applications.

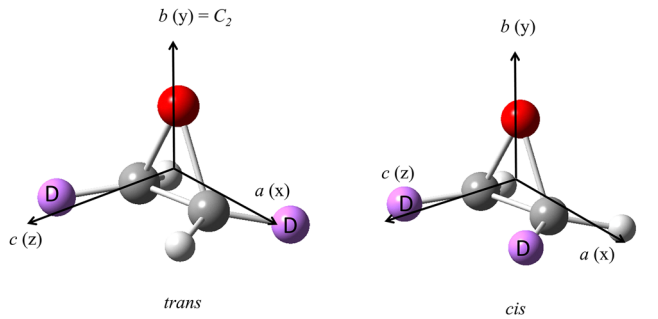


Fig. 1 Structures of the *trans* and *cis* isomers (carbon atoms are labeled in grey, hydrogen light grey, oxygen red and deuterium violet) with their principal axes *a*, *b*, *c* and axes definition for the rotational analysis. The $C_2$ axis in *trans*-2,3-dideutero-oxirane coincides with the *b*-axis. The (*R*,*R*)-2,3-dideutero-oxirane is shown here as one of the enantiomers of the *trans* isomer.

In a broader context, our spectroscopic results on monodeutero- and dideutero-oxirane should also be seen in relation to deuterium fractionation in astrochemistry. By these astrochemical processes deuterium is preferentially incorporated into a variety of molecules, the detection of which can then offer insight into these processes, which occur in particular in the cold and dense regions of interstellar space.[48–54] Despite the low cosmic abundance of deuterium with a ratio estimated to be about [D]/[H] $\approx 10^{-5}$, deuterium enriched molecules have been detected in various astronomical environments[51,52] with [D]/[H] ratios as high as 50% in low mass prestellar cores[53] and about 15% in protostars.[54] Such observations are crucial for refining models for chemical evolution in space, and in this context studies of deuterium fractionation in isotopically chiral molecules containing deuterium are also of greatest interest.

The undeuterated parent species oxirane (*c*-$C_2H_4O$) is an isomer of acetaldehyde ($CH_3CHO$) which is more stable by about 1 eV or 100 kJ mol$^{-1}$. The high-resolution spectroscopy of acetaldehyde[55] enabled its detection in the interstellar medium in the past.[56] The monodeutero isotopomer $CH_3CDO$ has also been detected in the ISM,[57] and interestingly dideuteroacetaldehyde $CHD_2CHO$ has recently been detected as well,[58] and tentatively also $CD_2CH_2O$[59] as isomers of *tc*-CHDCHDO. Clearly, the isotopomer $CD_3CHO$, which we studied some time ago in a different context,[60–62] would also be a candidate for future astrophysical observations. We might mention here also the isomers vinyl alcohol ($CH_2CHOH$) and methylhydroxycarbene ($CH_3COH$) and their isotopomers as further interesting candidates for a detection by astrophysical spectroscopy.

To complete this introduction, we should refer to the very extensive spectroscopic work which exists on normal achiral oxirane, quite in contrast to its isotopically chiral isotopomers. There are studies by microwave spectroscopy,[46,47,63,64] submillimetre wave spectroscopy,[65,66] and synchrotron-based FTIR spectroscopy.[67,68] As a result, the rotational parameters of the vibrational ground state of $C_2H_4O$ are extremely well established. The rovibrationally resolved infrared spectra of oxirane were also analysed in the range from 600 to 3500 cm$^{-1}$.[68–73] For comparison, extensive *ab initio* results are available as well, which include also results on deutero isotopomers.[21,38,74]

The present paper is organised as follows. In Section 2, we provide an overview over the experiments (synthesis, Section 2.1, GHz experiments Section 2.2, THz (FTIR) experiments Section 2.3). In Section 3, we briefly provide the theoretical background for the analysis (effective Hamiltonian Section 3.1, symmetry considerations for the analysis, Section 3.2). Section 4 discusses the assignment procedures and Section 5 provides results and discussion with the concluding Section 6 providing a summary of the main results and conclusions including an outlook. Some preliminary results of our work were presented in ref. 75 and 76. Because our sample of *tc*-CHDCHDO contained the achiral *cis*-CHDCHDO as an impurity, we were able to assign more than 1000 lines in the spectrum to this species,

 

and we report also the rotational parameters resulting from this analysis.

## 2. Experimental

### 2.1 Synthesis of di-deuterated oxirane

In brief, the synthesis of *trans-c*-$C_2H_2D_2O$ is described by the scheme below. The procedures can be presented as follows (Scheme 1):

**Dideuteroacetylene**[77]. Calcium carbide (30.0 g, 468 mmol) was placed in a flask and deuterium oxide >99.9 (atom % D) (10.0 mL, 562 mmol, 1.2 equiv.) was carefully added under water bath cooling. Dideuteroacetylene gas was collected in a 10-litre container.

GC-MS (EI): $m/z$ = 28.04 $[M]^+$, 26.06 $[M–D]^+$

**Dideuteroethylene**[78]. Chromium(III)chloride hexahydrate (159 g, 600 mmol, 1.50 equiv.) was dissolved in a solution of conc. hydrochloric acid (12.1 M, 100 mL) in water (200 mL). Zinc powder (52.3 g, 800 mmol, 2.00 equiv.) was slowly added while stirring, whereby a vigorous gas evolution took place. Dideuteroacetylene (6) (11.2 g, 400 mmol) was pumped through the solution with a gear pump for 4 h.

GC-MS (EI): $m/z$ = 30.15 $[M]^+$, 29.10 $[M–H]^+$, 28.12 $[M–D]^+$, 27.12 $[M–H–D]^+$

***rac*-[1,2-$^2H_2$]-2-Bromoethanol (*rac*-8)**[79]. Dideuteroethylene was pumped through an aqueous solution (500 mL) into which drops of bromine (15.5 mL, 303 mmol) were added over a period of four hours. The aqueous solution was extracted with diethylether (300 mL), potassium chloride was added (100 g) and extracted with ethylacetate. The solvents were removed under vacuum and the ether extract was purified by column chromatography ($SiO_2$, DCM, $R_f$ = 0.38).

$^1$H-NMR (500.13 MHz, $CDCl_3$): $\delta$ = 3.88–3.92 (m, 1H, 1-H), 3.50–3.54 (m, 1H, 2-H), 2.69 (bs, 1H, OH).

$^{13}$C-NMR (125.77 MHz, $CDCl_3$): $\delta$ = 62.29 (t, $J$ = 22.6 Hz), $\delta$ = 35.28 (t, $J$ = 22.6 Hz).

***rac*-1,2-Dideuterooxirane.** *rac*-[1,2-$^2H_2$]-2-Bromoethanol (14.1 g, 112 mmol) was placed in a flask provided with a dropping funnel, $N_2$ inlet and reflux cooler. The reflux cooler was equipped with a column filled with 3 Å molecular sieve connected to a cold trap filled with an ethanol/liquid $N_2$ mixture at −80 °C. An aqueous solution of 25% NaOH (47.5 mL) was slowly added under stirring and the reaction mixture was heated at 100 °C, passing a slow flow of $N_2$ gas through the apparatus. After three hours reaction time the product was obtained as a colourless liquid from the cold trap (4.33 g, 84%).

$^1$H-NMR (500.13 MHz, $CDCl_3$, −10 °C): $\delta$ = 2.70–2.71 (m, 2H, 1-H/2-H).

$^{13}$C-NMR (125.77 MHz, $CDCl_3$, −10 °C): $\delta$ = 40.7 (t, $J$ = 23.9 Hz).

GC-MS (EI): $m/z$ = 46.13 $[M]^+$, 44.08 $[M–D]^+$, 30.10 $[M–O]^+$, 29.09 $[M–O–H]^+$.

The reaction product contained mainly *tc*-CHDCHDO as racemate, with *cis*-CHDCHDO as an impurity. The identities of the substances were obvious from the high resolution spectra (see also ref. 19 and 21 for further aspects of the synthesis).

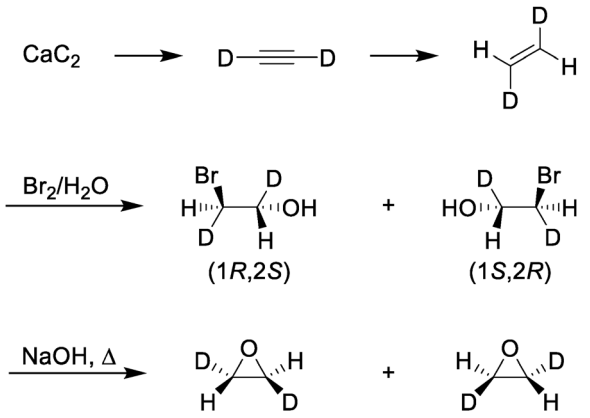


Scheme 1 The synthesis of *tc*-CHDCHDO.

### 2.2 GHz measurements

The rotational spectra of *trans*-2,3-dideutero-oxirane in the GHz region were recorded using our Zurich GHz spectrometer,[80] with some modifications which will be described elsewhere in more detail.[94] In this setup, the GHz radiation is phase modulated and sent through a 2.5 m long gas cell. Subsequently, the second harmonic is detected by a RF lock-in amplifier resulting in a derivative line shape from the absorption and dispersion of the gas sample. The high sensitivity of this setup has been demonstrated in our high-resolution spectroscopic studies of dithiine,[81] deuterated phenols[82] and monodeutero-oxirane.[19,21]

*Trans*-2,3-dideutero-oxirane was allowed to flow from the sample holder to the 2.5 m glass cell at optimised pressures between 9 and 30 μbar and room temperature. The survey spectra were initially recorded in the 95–105 GHz range in 500 MHz segments with a typical effective linewidth (FWHM, full-width at half-maximum) of ∼200 kHz observed at 100 GHz. Based on the rotational constants reported by Hirose,[47] transitions with decent intensities were assigned readily, leading to more accurate predicted line positions. Subsequently, longer integration times were applied to individual weaker transitions by selecting a narrow bandwidth (∼5 MHz) for the best signal-to-noise (S/N) ratio. Finally, the measurement of individual lines was extended to 64 GHz (lower limit) and 500 GHz (upper limit) to obtain better predictions through an improved effective Hamiltonian with additional transitions.

The relative frequency uncertainty of the GHz spectrometer is only $\Delta\nu/\nu = 10^{-11}$ and therefore the effective resolution and frequency accuracy is determined by Doppler and possible collisional effects as well as by the procedures used to extract peak positions of the lines (here also with the aid of PGOPHER[83,84]). The accuracy of an isolated line position has been tested with carbonylsulfide (OCS) and reaches at least 30 kHz or better. Through the derivative detection method, however, the maxima of two lines separated by more than one full-width at half-maximum (FWHM) can still be shifted in the

same order as the FWHM. Also, lines with stronger absorbance can have a deviation between line shape maximum and line position by more than 30 kHz, which is not always taken into account by the parameter extraction. Therefore, the frequency uncertainty for some lines might be as large as 200 kHz even though the root mean square deviation $d_{RMS}$ of the fit indicates an average precision of about 7 kHz. Therefore, these exceptional uncertainties have no significant effect on the analysis with the effective Hamiltonian. To minimise uncertainties, transitions in Table S3 have been remeasured separately at low pressures $<2$ μbar.

### 2.3 THz measurements

The far infrared beamline at the Swiss light source (SLS) was equipped with the ETH-SLS Bruker IFS 125 HR (extended) spectrometer, which was built as a prototype for our group in 2009 and is capable of measuring rotationally-resolved vibrational spectra in the THz range with an unapodized instrumental resolution of 0.00053 $cm^{-1}$ (16 MHz), the highest for an FTIR spectrometer of this type worldwide.[9,85–87] The combination of the high resolution of this prototype spectrometer with the high sensitivity enabled by the bright synchrotron radiation provides a powerful tool to measure and analyse the pure rotational transitions in the traditionally difficult THz region for FTIR spectroscopy. This capability was recently demonstrated by our successful study of the THz spectrum of monodeutero-oxirane.[19]

The pure rotational spectra in the range from 25 to 80 $cm^{-1}$ (0.75–2.40 THz) were measured with a maximum optical path difference $d_{MOPD}$ of 11.7 m. A 6 μm Mylar beamsplitter, an aperture of 3.15 mm and a helium-cooled Si bolometer were used for the measurements. The scanner velocity was 30 kHz. The measurements of the spectra started with a sample with a vapour pressure of 0.95 mbar with 140 interferograms collected. Further measurements were then conducted at two reduced pressures (166 and 140 scans, respectively), so that the line positions of strong but saturated transitions at the starting pressure were also accurately recorded. Fig. 2 shows an overview of the measured THz spectra of *trans*-2,3-dideutero-oxirane.

All measured line positions were calibrated using residual $H_2O$ vapour lines between 36 and 100 $cm^{-1}$ as compared to wavenumbers reported in the HITRAN database.[88] Based on a simple linear fit, the correction for the calibrated wavenumber $\tilde{\nu}_{calibrated} = 0.999999 \times \tilde{\nu}_{observed} + 0.000148$ $cm^{-1}$ is small enough to be taken as constant in this range. In general, the uncertainties of the recorded line positions can be estimated to be less than 0.0001 $cm^{-1}$. The wavenumber tables in the supplementary information (SI) give the calibrated values. The typical line widths $\Delta\tilde{\nu}_{FWHM}$ (full width at half-maximum, FWHM) were observed to be less than $\Delta\tilde{\nu}_{FWHM}$ = 0.0006 $cm^{-1}$, indicating that the resolution is instrument limited given the Doppler width of about 0.00009 $cm^{-1}$ at 50 $cm^{-1}$ and small pressure effects only. An example of an isolated line is shown in Fig. 2 as an insert (middle left).

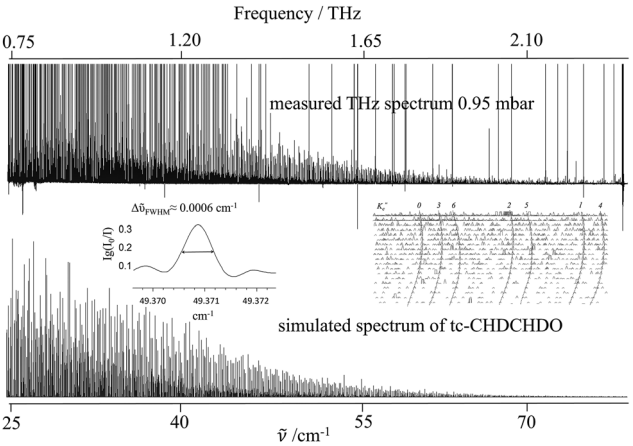


Fig. 2 An overview of the THz spectrum of *trans*-2,3-dideutero-oxirane (*tc*-CHDCHDO) between 0.75 and 2.4 THz. Along the ordinate axis, decadic absorbance $\lg(I_0/I)$ is shown where the cutoff at maximum absorbance has the value of 2, pathlength $l$ = 10 m, pressure = 0.95 mbar and temperature = 294 K. The middle left shows an example of the typical linewidth (full width at half-maximum) of about 0.0006 $cm^{-1}$ in the measured range, while the middle right is the Loomis–Wood diagram illustrating the patterns of transitions with common $K_c''$ values. The lower panel shows the simulated spectrum of *tc*-CHDCHDO at 294 K.

## 3. Theoretical background for the analysis

### 3.1 Effective Hamiltonian

The analyses of the pure rotational spectra in the GHz and THz regions were carried out using Watson's *A*-reduced effective Hamiltonian[89–93] in the $I^r$ representation, which is used here including up to octic centrifugal distortion constants:

$$\begin{aligned}\hat{H}^{v,v}_{rot} &= A_v\hat{J}_z^2 + B_v\hat{J}_x^2 + C_v\hat{J}_y^2 - \Delta_J^v\hat{J}^4 - \Delta_{JK}^v\hat{J}^2\hat{J}_z^2 - \Delta_K^v\hat{J}_z^4 \\ &\quad - \frac{1}{2}\left[\left(\delta_J^v\hat{J}^2 + \delta_K^v\hat{J}_z^2\right), \left(\hat{J}_+^2 + \hat{J}_-^2\right)\right]_+ + \phi_J^v\hat{J}^6 + \phi_{JK}^v\hat{J}^4\hat{J}_z^2 \\ &\quad + \phi_{KJ}^v\hat{J}^2\hat{J}_z^4 + \phi_K^v\hat{J}_z^6 \\ &\quad + \frac{1}{2}\left[\left(\eta_J^v\hat{J}^4 + \eta_{JK}^v\hat{J}^2\hat{J}_z^2 + \eta_K^v\hat{J}_z^4\right), \left(\hat{J}_+^2 + \hat{J}_-^2\right)\right]_+ \\ &\quad + L_J^v\hat{J}^8 + L_{JJK}^v\hat{J}^6\hat{J}_z^2 + L_{JK}^v\hat{J}^4\hat{J}_z^4 + L_{KKJ}^v\hat{J}^2\hat{J}_z^6 \\ &\quad + L_K^v\hat{J}^8 + \left[l_K^v\hat{J}^6, \left(\hat{J}_x^2 - \hat{J}_y^2\right)\right]_+ \\ &\quad + P_{KKJ}^v\hat{J}^2\hat{J}_z^8 + P_K^v\hat{J}^{10} + \left[p_K^v\hat{J}^8, \left(\hat{J}_x^2 - \hat{J}_y^2\right)\right]_+ \end{aligned} \quad (1)$$

where with $i = \sqrt{-1}$ we have the angular momentum operators:

$$\hat{J}^2 = \hat{J}_x^2 + \hat{J}_y^2 + \hat{J}_z^2 \quad (2)$$

$$\hat{J}_\pm = \hat{J}_x \pm i\hat{J}_y \quad (3)$$

The symbol $[,]_+$ stands for the anti-commutator and we prefer here the notation with the Greek $\eta$, because the also commonly used lower case Greek $\phi$ can be confused with the upper case $\Phi$.

 

### 3.2 Symmetry considerations

*Trans*-2,3-dideutero-oxirane is a highly asymmetric rotor of $C_2$ symmetry with an asymmetry parameter $\kappa = \frac{2B - A - C}{A - C} \approx 0.084$. Its permanent electric dipole moment is expected to lie along the $C_2$-symmetry ($b$)-axis allowing transitions obeying b-type selection rules (eo ↔ oe and ee ↔ oo, e for even and o for odd values of the quantum numbers $K_a$ and $K_c$)[90,91] with $\mu_b$ estimated to be similar to that of normal oxirane of 1.88 ± 0.01 D.[63,64] The principal axis systems for *trans*-2,3-dideutero-oxirane and *cis*-2,3-dideutero-oxirane are shown in Fig. 1, and Table 1 includes the character table for the point group $C_2$ and the molecular symmetry group $M_{S2}$ relevant for *tc*-CHDCHDO.

The nuclear spin statistical weights $g$ of *trans*-2,3-dideutero-oxirane arise from the nuclear spin functions of two protons ($I_H = 1/2$) and two deuterons ($I_D = 1$). For the main $^{12}C$ and $^{16}O$ species, the nuclear spin is zero for C and O. In total, there are $\Pi(2I_i + 1) = (2I_H + 1)(2I_H + 1)(2I_D + 1)(2I_D + 1) = 36$ nuclear spin functions. Because of the generalised Pauli principle[8] as applied to all particles involved here, the complete internal wave function of the molecule must be antisymmetric (or B in Table 1). This leads to the nuclear spin statistical weights $g$ for the rotational levels described by the combination $K_aK_c$ in the totally symmetric vibrational and electronic ground state as given in Table 1. Nuclear spin symmetry (A or B) is an approximately conserved property for the radiative transitions in our experiments, where we have not observed any transitions connecting the two nuclear spin isomers (A or B). As the rovibronic A and B levels are statistically equally abundant for this $C_2$-symmetric molecule,[95] the B isomer has the higher equilibrium concentration at room temperature, given the higher nuclear spin statistical weight 21 and, by convention called the *ortho*-isomer. The other isomer (A) with weight 15 is called the *para*-isomer, by the usual convention. Parity is not a good quantum number for *tc*-CHDCHDO, because the very high barrier for inversion at the C-atoms leads to a complete suppression of inversion tunnelling: the small $\Delta_{pv}E$ is many orders of magnitude larger than the hypothetical tunnelling splitting.[8–10] For further discussions of these symmetry aspects, see ref. 8–10 and 96.

## 4. Assignment of the pure rotational spectra in the ground state

The rotational spectra of *trans*-2,3-dideutero-oxirane in the GHz and THz ranges were first assigned and fitted independently, followed by a global analysis of all transitions measured in both ranges. As a result, a common set of spectroscopic parameters for the ground state was obtained.

The assignment of the GHz spectra was assisted by a simulation of the spectrum using the previously reported rotational constants in ref. 46 and 47, which were based on the analysis of 21 transitions with $J_{max} = 8$ and $K_{c\,max} = 4$. In our work, a total of 1413 b-type transitions were assigned using the PGOPHER program[83,84] in the range of 64–500 GHz with $J_{max} = 51$ and $K_{c\,max} = 34$. The newly assigned transitions were introduced into a least squares analysis and the resulting spectroscopic parameters are given in Table 2. In these analyses we used the programs WANG[92] and SPFIT,[93] giving essentially identical results. The root-mean-square deviation $d_{rms}$ of the fit is less than 8 kHz, with the typical linewidths (FWHM) of about 200 kHz in the GHz spectra. The rotational constants $A$, $B$ and $C$ are in good agreement with those previously determined by microwave spectroscopy.[47] Many higher order parameters are determined here for the first time.

The assignment of the THz spectrum was more challenging as transitions due to other species, likely by-products of the synthesis such as monodeutero-oxirane and normal oxirane, were present in the observed spectrum (see below). To ensure an unambiguous assignment, a cautious procedure was carried out: (1) a Loomis–Wood diagram[91,97,98] was constructed so that the regularly occurring patterns in several series were evident. The right insert in Fig. 2 shows progressions of transitions with common $K_c''$ values; (2) only isolated transitions in these series with strong intensities ($K_c \leq 8$ with $20 \leq J \leq 30$) were assigned initially; (3) these preliminary line positions were added to the line list together with the lines assigned in the GHz range, which are 70 times more heavily weighted; (4) thereafter further transitions were assigned and fitted, the simulated spectrum was refined, leading to the assignment of further transitions ($K_c \geq 8$ with $J \geq 30$). This iterative process was continued until all stronger transitions had been accounted for. An additional 2556 rotational transitions were assigned in the range of 0.75–2.4 THz (25 to 80 $cm^{-1}$). The range of quantum numbers of assigned transitions extends from $J = 17$ to 65 with $0 \leq K_c \leq 65$.

Ultimately, 4133 assigned line positions in the THz and GHz range and 21 lines reported by ref. 47 were co-fitted to obtain a common set of ground state spectroscopic parameters of *tc*-CHDCHDO. It turned out by inspection of the MW data from ref. 46 and 47 and the resulting fits that these had much larger uncertainties than most of the GHz lines reported in this study. Therefore, while presenting all known line data in Tables S1 and S2 in the SI, in the final best compromise fit we excluded some of the low frequency data (indicated by an asterisk * in the supplementary tables) in order to obtain a best estimate for the effective Hamiltonian parameters given in Tables 2 and 3. However, the results of a fit including all data are also given in the SI (Table S4). The differences between the parameters from the two fits are not large. In the global fit, the line frequencies assigned in the THz and GHz regions were weighted based on the linewidths of 0.2 MHz and 14 MHz, respectively, such that the greater precision of the GHz measurement is reflected in a

Table 1 Character tables for the $C_2$ and $M_{S2}$ symmetry groups (the symmetry assignment for $K_aK_c$ applies for a totally symmetric vibronic state)[a]

| | | $E$ | $C_2$ | | | |
|---|---|---|---|---|---|---|
| $C_2$ | $M_{S2}$ | $E$ | $(\alpha\beta)$ | $K_aK_c$ | $\mu$ | $g$ |
| A | A | 1 | 1 | ee, oo | $\mu_y$ | 15 |
| B | B | 1 | −1 | eo, oe | $\mu_x$, $\mu_z$ | 21 |

[a] $(\alpha\beta)$ is the simultaneous exchange of the CHD groups, $g$ is the nuclear spin statistical weight and $\mu_x$, $\mu_y$, $\mu_z$ are the electric dipole moment components.

Table 2 Spectroscopic parameters for the ground state of 2,3-dideuterooxirane in the GHz range in MHz (values in parentheses provide statistical 1$\sigma$ uncertainties in units of the last specified digits, see also discussions in the text)

| | *Trans*-2,3-dideutero-oxirane | | | *Cis*-2,3-dideutero-oxirane | | |
|---|---|---|---|---|---|---|
| | MW previous[a] | GHz (SP) | GHz (LP) | MW previous[a] | GHz (SP) | GHz (LP) |
| $A$/MHz | 22 943.19 | 22 943.193860(59) | 22 943.194100(58) | 22 700.41 | 22 700.415590(82) | 22 700.415740(78) |
| $B$/MHz | 18 198.47 | 18 198.503910(58) | 18 198.503910(53) | 18 318.39 | 18 318.511470(84) | 18 318.511380(78) |
| $C$/MHz | 12 585.27 | 12 585.291410(63) | 12 585.291390(57) | 12 650.08 | 12 650.101900(90) | 12 650.101810(83) |
| $\Delta_J$/kHz | — | 13.94040(20) | 13.94050(18) | — | 14.63690(42) | 14.63650(39) |
| $\Delta_K$/kHz | — | 24.423800(77) | 24.42600(14) | — | 24.16270(11) | 24.16540(22) |
| $\Delta_{JK}$/kHz | — | 14.379500(82) | 14.37910(11) | — | 12.31080(14) | 12.31010(22) |
| $\delta_j$/kHz | — | 3.568150(12) | 3.568160(11) | — | 3.846750(31) | 3.846760(28) |
| $\delta_k$/kHz | — | 9.739950(56) | 9.740000(52) | — | 9.002370(90) | 9.002100(87) |
| $\phi_J$/mHz | — | 6.00(19) | 6.00(18) | — | 9.70(61) | 9.00(57) |
| $\phi_{JK}$/mHz | — | 255.320(99) | 254.80(10) | — | 250.20(14) | 249.10(20) |
| $\phi_{KJ}$/mHz | — | −1174.10(18) | −1173.30(20) | — | −1177.50(25) | −1177.40(54) |
| $\phi_K$/mHz | — | 1086.01(11) | 1088.80(21) | — | 1087.50(17) | 1092.80(50) |
| $\eta_J$/mHz | — | 0.9530(73) | 0.9560(67) | — | 2.590(20) | 2.600(18) |
| $\eta_{JK}$/mHz | — | 108.490(56) | 108.500(51) | — | 111.270(92) | 110.960(90) |
| $\eta_K$/mHz | — | −120.170(84) | −120.000(77) | — | −130.20(11) | −130.10(10) |
| $L_{JK}$/Hz | — | — | 0.870(90) | — | — | 2.90(48) |
| $L_{KKJ}$/Hz | — | — | −2.30(15) | — | — | −5.30(47) |
| $d_{\mathrm{rms}}$/kHz | — | 7.380 | 6.710 | — | 6.573 | 5.986 |
| $N_{\mathrm{data}}$ | 21 | 1577 | 1577 | 22 | 1121 | 1121 |

[a] Ref. 47.

Table 3 Spectroscopic parameters for the ground state of deuterated oxiranes in MHz (values in parentheses provide statistical 1$\sigma$ uncertainties in units of the last specified digits)

| | *Cis*-2,3-dideutero-oxirane (GHz, SP) | Monodeutero-oxriane[a] (THz, GHz and mw) | *Trans*-2,3-dideutero-oxirane (GHz and THz, SP) | *Trans*-2,3-dideutero-oxirane (GHz and THz, LP) |
|---|---|---|---|---|
| $A$/MHz | 22 700.415590(82) | 24 252.64570(15) | 22 943.19366(12) | 22 943.19415(14) |
| $B$/MHz | 18 318.511470(84) | 19 905.52270(20) | 18 198.50392(10) | 18 198.50396(10) |
| $C$/MHz | 12 650.101900(90) | 13 327.58370(16) | 12 585.29181(11) | 12 585.29173(11) |
| $\Delta_J$/kHz | 14.63690(42) | 17.04117(26) | 13.94023(19) | 13.94027(19) |
| $\Delta_K$/kHz | 24.16270(11) | 25.45675(24) | 24.42401(22) | 24.42699(30) |
| $\Delta_{JK}$/kHz | 12.31080(14) | 17.25473(26) | 14.37793(21) | 14.37796(33) |
| $\delta_j$/kHz | 3.846750(31) | 4.741796(42) | 3.567874(34) | 3.567959(33) |
| $\delta_k$/kHz | 9.002370(90) | 13.23277(11) | 9.74110(15) | 9.74086(15) |
| $\phi_J$/mHz | 9.70(61) | 11.697(95) | 4.330(57) | 4.460(56) |
| $\phi_{JK}$/mHz | 250.20(14) | 138.67(17) | 253.41(25) | 253.34(30) |
| $\phi_{KJ}$/mHz | −1177.50(25) | −829.84(22) | −1171.00(50) | −1170.70(55) |
| $\phi_K$/mHz | 1087.50(17) | 797.41(14) | 1083.95(30) | 1087.90(49) |
| $\eta_J$/mHz | 2.590(20) | 4.602(15) | 0.784(18) | 0.832(18) |
| $\eta_{JK}$/mHz | 111.270(92) | 62.056(62) | 109.65(14) | 109.37(14) |
| $\eta_K$/mHz | −130.20(11) | 33.301(74) | −121.47(23) | −120.99(22) |
| $L_{JK}$/Hz | — | — | — | 0.95(24) |
| $L_{KKJ}$/Hz | — | — | — | −2.60(28) |
| $d_{\mathrm{rms}}$/kHz | 6.242 | 2679.7 | 1498.5 | 1467.4 |
| $N_{\mathrm{data}}$ | 1121 | 3370 | 4133 | 4133 |

[a] Ref. 21, Table 4 SP.

ratio of roughly 70 : 1. Table 2 compares also the result obtained with a small parameter set (SP) excluding octic parameters, and a larger parameter set, including some of the octic parameters ($L_{JK}$ and $L_{KKJ}$). It appears that the fit with the smaller parameter set is adequate for the present analysis. Table 3 presents the results from the global fit.

## 5. Results and discussion

Pure rotational transitions were measured and assigned in the GHz range from 64 to 500 GHz, allowing a much broader coverage of energy levels than in the previous microwave study.[47] This allowed for an accurate determination of the quartic ($\Delta_J$, $\Delta_K$, $\Delta_{JK}$, $\delta_j$, $\delta_k$), sextic ($\phi_K$, $\phi_J$, $\phi_{JK}$, $\phi_{KJ}$, $\eta_J$, $\eta_K$, $\eta_{JK}$), and some octic ($L_{JK}$, $L_{KKJ}$) centrifugal distortion parameters of the ground state of *tc*-CHDCHDO, which were not previously available, in addition to the now much more accurate rotational constants. The root-mean-square deviations of the fit of about 7 kHz is significantly smaller than one-tenth of the observed linewidths of ~200 kHz, indicating that the effective Hamiltonian used here provides an accurate description of the observed spectral features in this range. As a result, the simulation based

 

on the spectroscopic parameters in Table 2 reproduces the experimental spectra very well. Such comparisons are shown in Fig. 3–5.

For the analysis of the FTIR spectra consisting of transitions with higher $J$ and $K_c$ values in the THz range, further higher order parameters were used in the fit as shown in Table 3. The three measurements of THz spectra at different pressures allowed the recording of a large number of transitions with different intensities. A total of 2556 assigned transitions in the range from $J = 17$ to 65 with $0 \leq K_c \leq 65$ provided energy levels to accurately determine higher order parameters, to which the high $K_c$ lines are extremely sensitive. The transitions assigned in the GHz and THz range were finally fitted simultaneously. The $d_{rms}$ of this global fit is less than 1.5 MHz. Again, the fit with the small parameter set seems to be adequate also in comparison with a fit including some octic constants (LP). The low $d_{rms}$ is further evidence of the excellent representation of the observed spectra by the effective Hamiltonian used. Fig. 4 shows the comparison between the observed THz spectrum and the simulation based on the spectroscopic parameters given in Table 3.

In addition to the lines assigned to *tc*-CHDCHDO, additional lines were observed in the GHz spectrum as shown in Fig. 3. Many of these transitions could be attributed to *cis*-2,3-dideutero-oxirane (1121 new transitions were assigned, see Table 2 for the resulting spectroscopic parameters), monodeutero-oxirane[21] and normal oxirane[67,68,70] as by-products of the synthesis firmly established as based on the available high-resolution data. In the THz region, the spectral overlap is much more pronounced, and it is evident from Fig. 4

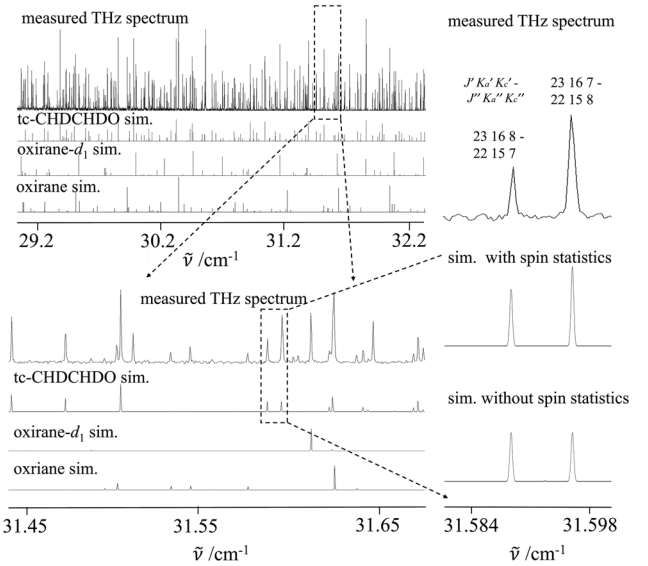


Fig. 4 A comparison of observed and simulated rotational spectra of *trans*-2,3-dideutero-oxirane (*tc*-CHDCHDO), monodeutero-oxirane ($C_2H_3DO$) and normal oxirane (*c*-$C_2H_4O$) in the THz region. Decadic absorbance $\lg(I_0/I)$ is shown on the ordinate where the cutoff at maximum absorbance has the value of 0.9, pathlength $l$ = 10 m, pressure = 0.95 mbar and temperature = 294 K. The right panel shows an enlarged section with the simulation of the spectra of *tc*-CHDCHDO with (middle trace) and without (lower trace) nuclear spin statistics.

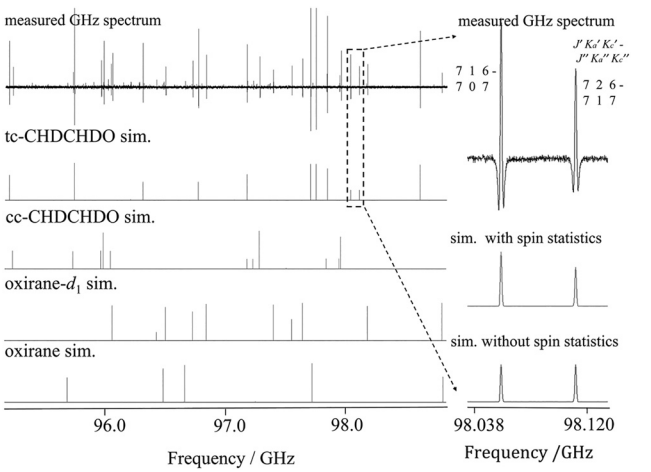


Fig. 3 A comparison of observed and simulated rotational spectra in the GHz region. From top to bottom: (1) experimental spectrum with pressure = 25 μbar and temperature = 294 K; (2) simulation of *trans*-2,3-dideutero-oxirane (*tc*-CHDCHDO); (3) simulation of *cis*-2,3-dideutero-oxirane (*cc*-CHDCHDO); (4) simulation of monodeutero-oxirane (oxirane-$d_1$) using spectroscopic parameters from ref. 21; (5) simulation of normal oxirane using spectroscopic parameters from ref. 67 and 68. The right panel shows an enlarged section with the simulation of the spectra of *tc*-CHDCHDO with (middle trace) and without nuclear spin statistics (lower trace) with quantum numbers defined as $J' K_a' K_c' - J'' K_a'' K_c''$.

that no more than half of the observed lines are due to *trans*-2,3-dideutero-oxirane, while the remainder are due to other compounds such as monodeutero-oxirane, *cis*-2,3-dideutero-oxirane and normal oxirane. Therefore, we introduced a routine that adds only strong, isolated lines in a series in the Loomis–Wood diagram to the line list while co-fitting these transitions with the GHz lines, which are weighted 70 times more heavily in the preliminary assignment, so that accidental misassignments arising from overlapping lines arising from other species can be avoided. As the Hamiltonian model was improved after each iteration, we were gradually able to assign almost all predicted lines between 25 to 80 cm$^{-1}$, except for overlapped lines. Tables 2 and 3 also summarise the results for *cis*-2,3-dideutero-oxirane, which could be obtained from the "impurity" lines in a similar fashion.

It was possible to observe the intensity alternation in the spectra due to the nuclear spin statistical weights (Table 1). Fig. 3 and 4 show examples of a comparison of *tc*-CHDCHDO transitions with simulations with (right panel, upper trace) and without (right panel, lower trace) nuclear spin statistical weights in both the GHz and THz regions. Even for such a dense spectrum, the intensity alternation due to the different nuclear spin statistical weights for the nuclear spin isomers (A and B) is obvious, and confirms the assignments. Moreover, such intensity profiles play a crucial role in distinguishing this molecule from the other deuterated species in the sample, especially when dense spectra are observed. Interestingly, the presence of impurities in our sample illustrated the power of high-resolution spectroscopy in unambiguously identifying

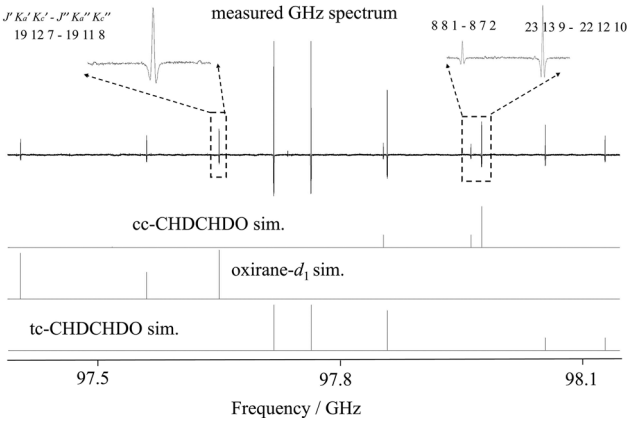


Fig. 5 A comparison of observed and simulated rotational spectra in the GHz region. From top to bottom: (1) experimental spectrum, pressure = 25 μbar and temperature = 294 K; (2) simulation of *cis*-2,3-dideutero-oxirane (*cc*-CHDCHDO); (3) simulation of monodeutero-oxirane ($C_2H_3DO$) using spectroscopic parameters from ref. 21; (4) simulation of *trans*-2,3-dideutero-oxirane (*tc*-CHDCHDO). Some lines of oxirane-$d_1$ and *cc*-CHDCHDO are shown magnified in the inserts with their assignments (see also Fig. 3).

molecules in such a mixture. More specifically, it provides the possibility to distinguish the spectra of oxirane and its isotopomers, which would be a likely scenario in field and astrophysical observations. Fig. 5 shows an enlarged section from Fig. 3, where the inserts show details of the weaker lines as assigned to mondeutero-oxirane and *cis*-dideutero-oxirane, which are clearly separated from the dominant *tc*-CHDCHDO lines.

The laboratory spectroscopy of both *cis*- and *trans*-2,3-dideutero-oxirane presented in this study provides important data that can significantly help in its possible detection in the ISM. The accurate determination of the rotational parameters allows for a precise prediction of the spectral line positions that can be targeted in astronomical observations. Given the recent discovery of mono-deutero-oxirane in the low-mass protostar IRAS 16 293–2422 B,[20] it is plausible that 2,3-dideutero-oxirane could also be detected in similar environments. The key to its detectability lies in its large dipole moment, which plays a crucial role in its radio astronomical signature. Table 4 provides a small selection of lines, which can be predicted to be possibly useful for such a detection and Table S3 in the SI provides a more extended list. In any case, the very accurate parameters of the effective Hamiltonian derived here allow for an accurate prediction of rotational transitions in the complete spectral range covered by our results from the low GHz up to 2 THz. Fig. 6 shows a further detailed section of the spectra from the range 330 to 360 GHz, which has been important for the detection of $CD_2CH_2O$[59] and $CHD_2CHO$[58] as isomers of *tc*-CHDCHDO.

## 6. Conclusions and outlook

The combination of highest resolution synchrotron based FTIR spectroscopy[9,85–87] in the difficult THz range with high precision GHz spectroscopy in our laboratory[80–82] enabled us here to obtain an accurate effective rotational Hamiltonian for the chiral *trans*-2,3-dideutero-oxirane and its achiral isotopomer *cis*-2,3-dideutero-oxirane in the vibrational ground state. Our analysis of the rotational spectra of these molecules covered a wide frequency range from about 60 GHz to more than 2 THz. The most obvious application of these results concerns astrophysical spectroscopy, where our results may lead to a detection of these molecules in the interstellar medium (ISM), given the very accurate rotational line results and predictions, the large dipole moments of these species and the previous detection of oxirane and monodeutero-oxirane.[13–21] From such observations one can expect important information on the processes of deuterium fractionation in the formation of isotopically chiral molecules, in particular, of which so far only one example, monodeutero-oxirane,[19–21] has been detected in

Table 4 Predicted frequencies of some promising transitions (in MHz) of *trans*-2,3-dideutero-oxirane to be found in the range of 330 to 360 GHz at 120 K based on the spectroscopic parameters reported in Table 2 GHz (SP) using transitions listed in Table S1. Some of those lines are shown in Fig. 6. The last column gives the lower state energies for the transitions in terms of $E''$/(h MHz)

| $J'$ | $K'_a$ | $K'_c$ | $J''$ | $K''_a$ | $K''_c$ | Predicted frequency | Observed frequency | $E''$/(h MHz) |
|---|---|---|---|---|---|---|---|---|
| 7 | 3 | 4 | 6 | 2 | 5 | 335 574.637 | 335 574.643 | 656 997.870 |
| 12 | 2 | 10 | 11 | 3 | 9 | 340 189.481 | 340 189.480 | 2 046 732.696 |
| 12 | 3 | 10 | 11 | 2 | 9 | 340 197.669 | 340 197.673 | 2 046 725.981 |
| 8 | 7 | 2 | 7 | 6 | 1 | 345 710.989 | 345 710.989 | 1 146 529.094 |
| 8 | 7 | 1 | 7 | 6 | 2 | 346 055.873 | 346 055.872 | 1 146 260.690 |
| 13 | 1 | 12 | 12 | 2 | 11 | 350 030.212 | 350 030.222 | 2 228 872.264 |
| 13 | 2 | 12 | 12 | 1 | 11 | 350 030.245 | 350 030.222 | 2 228 872.234 |
| 7 | 5 | 3 | 6 | 2 | 4 | 351 902.080 | 351 902.086 | 719 670.023 |
| 14 | 0 | 14 | 13 | 1 | 13 | 359 933.472 | 359 933.474 | 2 389 201.061 |
| 14 | 1 | 14 | 13 | 0 | 13 | 359 933.472 | 359 933.474 | 2 389 201.061 |
| 7 | 2 | 5 | 6 | 1 | 6 | 362 046.505 | 362 046.512 | 574 102.527 |
| 8 | 4 | 4 | 7 | 3 | 5 | 363 509.178 | 363 509.175 | 937 797.007 |

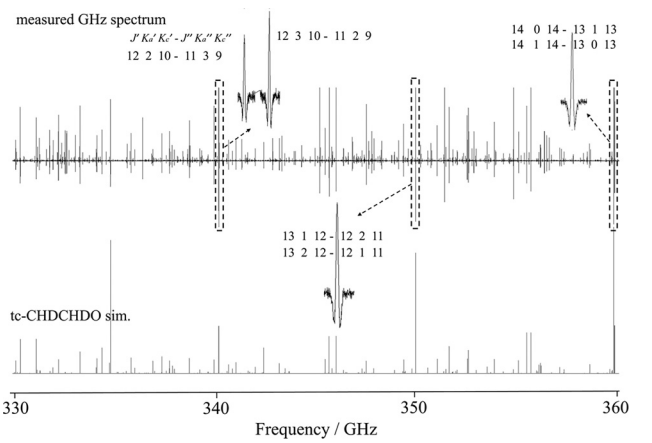


Fig. 6 A comparison of the observed spectrum at 30 μbar and simulated rotational spectra of *trans*-2,3-dideutero-oxirane (*tc*-CHDCHDO) in the range of 330 to 360 GHz at 294 K. Inserts show some of the transitions (quantum numbers defined as $J'K'_aK'_c - J''K''_aK''_c$) measured at reduced pressures below 2 μbar, which are among promising candidates for astrophysical searches listed in Table 4 and Table S3.

 

the ISM. Indeed, only two chiral molecules overall have so far been detected by astrophysical spectroscopy, with one additional example methyloxirane,[28,99] thus there is a great gap in our knowledge of the prevalence of chiral molecules in space outside the Earth. Our present work aims at helping to close this gap.

However, this is by no means the only possible application of our results. Apart from the obvious use for improving the structural information on the important prototype molecule oxirane ($C_2H_4O$), even of industrial relevance, *tc*-CHDCHDO is also an interesting candidate for the study of vibrational quantum dynamics of highly excited states by high resolution infrared spectroscopy,[60,61,91,100] for which the present accurate ground state parameters provide a starting point. Indeed, this chiral molecule has two ''isolated CH-chromophores'' separated by a C–C bond, and the quantum dynamics of vibrational energy transfer across bonds[101–103] in this kind of molecules is of great interest, with little knowledge available so far for such chiral systems. When combined with the study of time-dependent vibrational circular dichroism, it would presumably provide the first example of this kind hypothesized a longer time ago already.[3,101,104] One should furthermore consider the interesting expected differences in vibrational energy flow with respect to the isomer $CHD_2$–CHO[58] with two isolated CH-chromophores involving a slightly different chemical environment with an aldehydic CH-chromophore.[60–62] The extension of our work on *tc*-CHDCHDO to high resolution vibrational–rotational spectroscopy is in progress, similar to monodeutero-oxirane[21] and has also possible astrophysical applications with the recent successful launch of the James Webb telescope.[105–108]

Isotopically chiral molecules such as *tc*-CHDCHDO are also of obvious interest in relation to the fundamental physics of parity violation and tunnelling in chiral molecules.[2,9,10] $C_2$-symmetric molecules theoretically studied so far include HOOH,[109,110] HSSH,[111] where tunnelling dominates, but also ClSSCl[96,112] and 1,2-dithiine,[81] for example, where parity violation dominates and tunnelling is completely suppressed in the ground state. *tc*-CHDCHDO clearly is expected to fall in the latter class of molecules where chirality is completely dominated by parity violation, but a more quantitative theoretical study would be of interest. We should emphasise, though, that because of the qualitatively expected,[10] although so far not quantitatively calculated very small value of $\Delta_{pv}E$ for *tc*-CHDCHDO ($<1$ aeV), this molecule would not be a priority choice for measurements of $\Delta_{pv}E$. In this context 1,2-dithiine ($C_4H_4S_4$),[81] with a predicted $\Delta_{pv}E \approx 1.3$ feV or among substituted oxiranes fluoro-oxirane (21.1 aeV)[113–115] or cyano-oxirane (12.4 aeV)[99,116] would be more favourable candidates.

Returning to the perhaps most inspiring question of possible investigations on extraterrestrial homochirality in relation to the origin of life, accurate spectroscopic results on chiral molecules like the present one provide an early step towards such studies.[22,117] In contrast to other ''chemical-analytical'' approaches,[24] astrophysical spectroscopy is not limited to the solar system, one can, indeed, reach far out to other stars and galaxies.[117,118] While the complexity of life in relation to biomolecular homochirality presumably requires biopolymers such as proteins and DNA, not easily detected by gas phase spectroscopy in astrophysics, small chiral molecules can possibly be used as ''tracers'' for homochirality to be studied by chirally sensitive high resolution spectroscopy (circular dichroism, vibrational circular dichroism, Raman optical activity…, with observations on satellites to be planned for the future). While results along these lines are not expected in the nearest future, they could address some of the most fundamental open questions in science concerning the existence and prevalence of extraterrestrial life in the first place. This would be followed by the further open question, whether the given selection of homochirality (if any) is ''*de facto*'' (by chance, resulting in a statistical distribution over many different homochiralities) or ''*de lege*'' (by necessity, resulting in a preference of one, such as ours with L-aminoacids and D-sugars).[2,22,119–121] With high resolution spectroscopic results on chiral molecules such as presented here, one has a very early step towards answering such questions, although clearly very many further steps will be required.

## Conflicts of interest

There are no conflicts to declare.

## Data availability

Relevant data including lists of all transitions assigned are provided in the supplementary information (SI). Supplementary information is available. See DOI: **https://doi.org/10.1039/d5cp03143e**.

## Acknowledgements

We are indebted to Philippe Lerch for help in the earlier experiments. Help from and discussions with Carine Manca Tanner, Georg Seyfang and Jürgen Stohner and continuous support from Frédéric Merkt are gratefully acknowledged. This research was funded by ETH Zürich, in particular the LPC and the IMPS, the Swiss National Science Foundation (40-B2-0218759/Bridge), an ERC Advanced Grant as well as the COST projects MOLIM and COSY and the Fundamental Research Funds for Chinese Central Universities (No. lzujbky-2018-k08, lzujbky-2019-65 and lzujbky-2019-ct05). The research leading to these results has in particular also received funding from the European Union's seventh Framework Program (FP7/2007-2013) ERC grant agreement No. 290925. With deep gratitude we dedicate this publication to Jürgen Troe on the occasion of his 85th birthday 2025. He was involved in the foundation of PCCP and is a member of its honorary board, and he also has made fundamental contributions to the understandings of interstellar chemistry (see ref. 122).

## References


1 E. Babaev, D. Kharzeev, M. Larsson, A. Molochkov and V. Zhaunerchyk, Eds., Chiral Matter, Proceedings of the Nobel Symposium 167, Lidingö (Stockholm) 28 June to 2 July 2021, pp. 209–268; ed. E. Babaev, D. Kharzeev, M. Larsson, A. Molochkov, V. Zhaunerchyk, World Scientific Publishing Co, Singapore, 2023.

2 M. Quack, *Angew. Chem.*, 1989, **101**, 588; M. Quack, *Angew. Chem., Int. Ed. Engl.*, 1989, **28**, 571.

3 A. Beil, D. Luckhaus, R. Marquardt and M. Quack, *Faraday Discuss.*, 1994, **99**, 49.

4 R. Berger, M. Quack, A. Sieben and M. Willeke, *Helv. Chim. Acta*, 2003, **86**, 4048.

5 R. Berger, G. Laubender, M. Quack, A. Sieben, J. Stohner and M. Willeke, *Angew. Chem.*, 2005, **117**, 3689; R. Berger, G. Laubender, M. Quack, A. Sieben, J. Stohner and M. Willeke, *Angew. Chem., Int. Ed.*, 2005, **44**, 3623.

6 M. Hippler and M. Quack, Isotope Selective Infrared Spectroscopy and Intramolecular Dynamics, in *Isotope Effects in Chemistry and Biology, Part III Isotope Effects in Chemical Dynamics*, ed. A. Kohen and H.-H. Limbach, Marcel Dekker Inc., New York, 2005, pp. 305–359.

7 M. Hippler, E. Miloglyadov, M. Quack and G. Seyfang, Mass and Isotope Selective Infrared Spectroscopy, in *Handbook of High-Resolution Spectroscopy*, ed. M. Quack and F. Merkt, Wiley, Chichester, 2011, vol. 2, ch. 28, pp. 1069–1118, ISBN-13:978-0-470-06653-9.

8 M. Quack, Fundamental Symmetries and Symmetry Violations from High Resolution Spectroscopy, in *Handbook of High-Resolution Spectroscopy*, ed. M. Quack and F. Merkt, Wiley, Chichester, 2011, vol. 1, ch. 18, pp. 659–722, ISBN-13:978-0-470-06653-9.

9 M. Quack, G. Seyfang and G. Wichmann, Parity Violation in Chiral Molecules: From Theory, towards Spectroscopic Experiment and the Evolution of Biomolecular Homochirality, in 'Chiral Matter', Proceedings of the Nobel Symposium 167, Lidingö (Stockholm) 28 June to 2 July 2021, ed. E. Babaev, D. Kharzeev, M. Larsson, A. Molochkov and V. Zhaunerchyk, World Scientific Publishing Co, Singapore, 2023, pp. 209–268 (after lecture M. Quack).

10 M. Quack, G. Seyfang and G. Wichmann, *Chem. Sci.*, 2022, **13**, 10598.

11 M. Quack, *Chem. Phys. Lett.*, 1986, **132**, 147.

12 P. Dietiker, E. Miloglyadov, M. Quack, A. Schneider and G. Seyfang, *J. Chem. Phys.*, 2015, **143**, 244305.

13 J. E. Dickens, W. M. Irvine, M. Ohishi, M. Ikeda, S. Ishikawa, A. Nummelin and A. Hjalmarson, *Astrophys. J.*, 1997, **489**, 753.

14 A. Nummelin, J. E. Dickens, P. Bergman, A. Hjalmarson, W. M. Irvine, M. Ikeda and M. Ohishi, *Astron. Astrophys.*, 1998, **337**, 275.

15 M. Ikeda, M. Ohishi, A. Nummelin, J. E. Dickens, P. Bergman, A. Hjalmarson, W. M. Irvine and S. Ishikawa, *Astrophys. J.*, 2001, **560**, 792.

16 M. A. Requena-Torres, J. Martín-Pintado, S. Martín and M. R. Morris, *Astrophys. J.*, 2008, **672**, 352.

17 J. K. Jørgensen, M. H. D. van der Wiel, A. Coutens, J. M. Lykke, H. S. P. Müller, E. F. van Dishoeck, H. Calcutt, P. Bjerkeli, T. L. Bourke, M. N. Drozdovskaya, C. Favre, E. C. Fayolle, R. T. Garrod, S. K. Jacobsen, K. I. Öberg, M. V. Persson and S. F. Wampfler, *Astron. Astrophys.*, 2016, **595**, A117.

18 J. M. Lykke, A. Coutens, J. K. Jørgensen, M. H. D. van der Wiel, R. T. Garrod, H. S. P. Müller, P. Bjerkeli, T. L. Bourke, H. Calcutt, M. N. Drozdovskaya, C. Favre, E. C. Fayolle, S. K. Jacobsen, K. I. Öberg, M. V. Persson, E. F. van Dishoeck and S. F. Wampfler, *Astron. Astrophys.*, 2017, **597**, A53.

19 S. Albert, Z. Chen, K. Keppler, P. Lerch, M. Quack, V. Schurig and O. Trapp, *Phys. Chem. Chem. Phys.*, 2019, **20**, 3669.

20 H. S. P. Müller, J. K. Jorgensen, J.-C. Guillemin, F. Lewen and S. Schlemmer, *Mon. Not. R. Astron. Soc.*, 2023, **518**(1), 185.

21 S. Albert, Z. Chen, K. Keppler, G. Wichmann, M. Quack, V. Schurig and O. Trapp, *Phys. Chem. Chem. Phys.*, 2025, **27**, 14240.

22 M. Quack, *Adv. Chem. Phys.*, 2015, **157**, 249.

23 M. Quack, *Faraday Discuss.*, 2011, **150**, 533.

24 A. C. Evans, C. Meinert, J. H. Bredehoft, C. Giri, N. C. Jones, S. V. Hoffmann and U. J. Meierhenrich, Top. Curr. Chem., in *Differentiation of Enantiomers II*, ed. V. Schurig, notably section 4, The Rosetta mission and the COSAC experiment, Springer-Verlag, Berlin, Heidelberg, 2013, vol. 341, pp. 271–300.

25 X. Bonfils, X. Delfosse, S. Udry, T. Forveille, M. Mayor, C. Perrier, F. Bouchy, M. Gillon, C. Lovis, F. Pepe, D. Queloz, N. C. Santos, D. Ségransan and J.-L. Bertaux, *Astron. Astrophys.*, 2013, **549**, A109.

26 N. Madhusudhan, *Annu. Rev. Astron. Astrophys.*, 2019, **57**, 617.

27 S. Rukdee, *Sci. Rep.*, 2024, **14**, 27356.

28 Y. Ellinger, F. Pauzat, A. Markovits, A. Allaire and J.-C. Guillemin, *Astron. Astrophys.*, 2020, **633**, A49.

29 T. B. Freedman, M. G. Paterlini, N.-S. Lee, L. A. Nafie, J. M. Schwab and T. Ray, *J. Am. Chem. Soc.*, 1987, **109**, 4727.

30 T. B. Freedman, K. M. Spencer, N. Ragunathan, L. A. Nafie, J. A. Moore and J. M. Schwab, *Can. J. Chem.*, 1991, **69**, 1619.

31 K. J. Jalkanen, P. J. Stephens, R. D. Amos and N. C. Handy, *J. Am. Chem. Soc.*, 1988, **110**, 2012.

32 R. Dutler and A. Rauk, *J. Am. Chem. Soc.*, 1989, **111**, 6957.

33 P. J. Stephens, K. J. Jalkanen and R. W. Kawiecki, *J. Am. Chem. Soc.*, 1990, **112**, 6518.

34 P. L. Polavarapu and P. K. Bose, *J. Chem. Phys.*, 1990, **93**, 7524.

35 P. J. Stephens, K. J. Jalkanen, F. J. Devlin and C. F. Chabalowski, *J. Phys. Chem.*, 1993, **97**, 6107.

36 K. L. Bak, P. Jørgensen, T. Helgaker and K. Ruud, *Faraday Discuss.*, 1994, **99**, 121(see also discussion M. Quack pp. 98–99, 200–201, K. L. Bak pp. 201 herein).


 

37 K. L. Bak, O. Bludský and P. Jørgensen, *J. Chem. Phys.*, 1995, **103**, 10548.
38 V. Barone, M. Biczysko, J. Bloino and C. Puzzarini, *J. Chem. Phys.*, 2014, **141**, 034107.
39 P. Herwig, K. Zawatzky, M. Grieser, O. Heber, B. Jordon-Thaden, C. Krantz, O. Novotný, R. Repnow, V. Schurig, D. Schwalm, Z. Vager, A. Wolf, O. Trapp and H. Kreckel, *Science*, 2013, **342**, 1084.
40 P. Herwig, K. Zawatzky, D. Schwalm, M. Grieser, O. Heber, B. Jordon-Thaden, C. Krantz, O. Novotný, R. Repnow, V. Schurig, Z. Vager, A. Wolf, O. Trapp and H. Kreckel, *Phys. Rev. A:At., Mol., Opt. Phys.*, 2014, **90**, 052503.
41 K. Zawatzky, P. Herwig, M. Grieser, O. Heber, B. Jordon-Thaden, C. Krantz, O. Novotný, R. Repnow, V. Schurig, D. Schwalm, Z. Vager, A. Wolf, H. Kreckel and O. Trapp, *Chem. – Eur. J.*, 2014, **20**, 5555.
42 O. Trapp and K. Zawatzky, *Isr. J. Chem.*, 2016, **56**, 1082.
43 M. Pitzer, M. Kunitski, A. S. Johnson, T. Jahnke, H. Sann, F. Sturm, L. P. H. Schmidt, H. Schmidt-Böcking, R. Dörner, J. Stohner, J. Kiedrowski, M. Reggelin, S. Marquardt, A. Schießer, R. Berger and M. S. Schöffler, *Science*, 2013, **341**, 1096.
44 J. M. Bijvoet, A. F. Peerdeman and A. J. van Bommel, *Nature*, 1951, **168**, 271.
45 J. D. Dunitz, *X-ray Analysis and the Structure of Organic Molecules*, Cornell University Press, Ithaca and London, 1979.
46 C. Hirose, *Astrophys. J.*, 1974, **189**, L145.
47 C. Hirose, *Bull. Chem. Soc. Jpn.*, 1974, **47**, 1311.
48 E. Herbst, Deuterium Fractionation in Interstellar Space, *ACS Symposium Series*, 1992, vol. 502, ch. 22, pp. 358–368.
49 A. G. C. Tielens, *Rev. Mod. Phys.*, 2013, **85**, 1021.
50 J. L. Linsky, *Space Sci. Rev.*, 2003, **106**, 49.
51 C. Ceccarelli, *Planet. Space Sci.*, 2002, **50**, 1267.
52 E. Roueff and M. Gerin, *Space Sci. Rev.*, 2003, **106**, 61.
53 B. Parise, C. Ceccarelli, A. G. G. M. Tielens, E. Herbst, B. Lefloch, E. Caux, A. Castets, I. Mukhopadhyay, L. Pagani and L. Loinard, *Astron. Astrophys.*, 2002, **393**, L49.
54 P. Bergman, B. Parise, R. Liseau and B. Larsson, *Astron. Astrophys.*, 2011, **527**, 39.
55 A. Bauder and H. H. Günthard, *J. Mol. Spectrosc.*, 1976, **60**, 290.
56 W. Gilmore, M. Morris, D. R. Johnson, F. J. Lovas, B. Zuckerman and B. E. Turner, *Astrophys. J.*, 1976, **204**, 43.
57 J. K. Jørgensen, H. S. P. Müller, H. Calcutt, A. Coutens, M. N. Drozdovskaya, K. I. Öberg, M. V. Persson, V. Taquet, E. F. van Dishoeck and S. F. Wampfler, *Astron. Astrophys.*, 2018, **620**, A170.
58 J. Ferrer Asensio, S. Spezzano, L. H. Coudert, V. Lattanzi, C. P. Endres, J. K. Jørgensen and P. Caselli, *Astron. Astrophys.*, 2023, **670**, A177.
59 H. S. P. Müller, J. K. Jorgensen, J.-C. Guillemin, F. Lewen and S. Schlemmer, *J. Mol. Spectrosc.*, 2023, **394**, 111777.
60 A. Amrein, H. Hollenstein, M. Quack, R. Zenobi, J. Segall and R. N. Zare, *J. Chem. Phys.*, 1989, **90**, 3944.
61 M. Quack and J. Stohner, *J. Phys. Chem.*, 1993, **97**, 12574.
62 T. K. Ha, M. Quack and J. Stohner, *Mol. Phys.*, 2002, **100**, 1797.
63 G. Cunningham Jr., A. W. Boyd, R. J. Myers, W. D. Gwinn and W. I. Le Van, *J. Chem. Phys.*, 1951, **19**, 676.
64 R. A. Creswell and R. H. Schwendeman, *Chem. Phys. Lett.*, 1974, **27**, 521.
65 L. Pan, S. Albert, K. V. L. N. Sastry, E. Herbst and F. C. De Lucia, *Astrophys. J.*, 1998, **499**, 517.
66 D. T. Petkie, T. M. Goyette, R. P. A. Bettens, S. P. Belov, S. Albert, P. Helminger and F. C. De Lucia, *Rev. Sci. Instrum.*, 1997, **68**, 1675.
67 C. Medcraft, C. D. Thompson, E. G. Robertson, D. R. T. Appadoo and D. McNaughton, *Astrophys. J.*, 2012, **753**, 18.
68 S. Albert, K. Keppler Albert and M. Quack, in Proc. 22nd Colloquium on High Resolution Molecular Spectroscopy, Dijon, France 29 August – 2 September, 2011, H12, The high resolution FTIR spectrum of oxirane (ethyleneoxide, $C_2H_4O$): Rovibrational analysis of the $A_1$ fundamental $\nu_5$.
69 D. K. Russel and R. Wesendrup, *J. Mol. Spectrosc.*, 2003, **217**, 59.
70 F. Kwabia Tchana, J.-M. Flaud, W. J. Lafferty and M. Ngom, *Mol. Phys.*, 2014, **112**, 1633.
71 J.-M. Flaud, W. J. Lafferty, F. Kwabia Tchana, A. Perrin and X. Landsheere, *J. Mol. Spectrosc.*, 2012, **271**, 38.
72 W. J. Lafferty, J. M. Flaud, F. Kwabia Tchana and J. M. Fernandez, *Mol. Phys.*, 2013, **111**, 1983.
73 F. Kwabia Tchana, M. Ngom, A. Perrin, J.-M. Flaud, W. J. Lafferty, S. A. Ndiaye and El. A. Ngom, *J. Mol. Spectrosc.*, 2013, **292**, 1.
74 C. Puzzarini, M. Biczysko, J. Bloino and V. Barone, *Astrophys. J.*, 2014, **785**, 107.
75 Z. Chen, S. Albert, K. Keppler, M. Quack, V. Schurig and O. Trapp, Proc. 2021 Int. Symposium on Molecular Spectroscopy, Urbana, IL, USA, paper WJ01, 2021.
76 Z. Chen, S. Albert, K. Keppler, M. Quack, V. Schurig and O. Trapp, *International Workshop on Molecular Quantum Dynamics and Kinetics "Molecules in Motion" MOLIM2018, p35 – Academy of Athens, Athens, Greece, October 8 – 10, 2018*, ed. F. Merkt, M. Quack, I. Thanopulos and C. G. Vayenas, Athens, 2018 (PCCP Prize paper).
77 P. P. Nicholas and R. T. Carroll, *J. Org. Chem.*, 1968, **33**, 2345.
78 W. Traube and W. Passarge, *Chem. Ber.*, 1916, **49**, 1692.
79 C. P. Casey and L. J. Smith, *Organometallics*, 1989, **8**, 2288.
80 M. Suter and M. Quack, *Appl. Opt.*, 2015, **54**, 4417.
81 S. Albert, I. Bolotova, Z. Chen, C. Fabri, L. Horny, M. Quack, G. Seyfang and D. Zindel, *Phys. Chem. Chem. Phys.*, 2016, **18**, 21976.
82 S. Albert, Z. Chen, C. Fabri, P. Lerch, R. Prentner and M. Quack, *Mol. Phys.*, 2016, **114**, 2751–2768.
83 C. M. Western, *PGOPHER version 9.1*, University of Bristol Research Data Repository, 2016, DOI: **10.5523/bris.1nz94wvrfzzdo1d67et0t4v4nc**.
84 C. M. Western, Introduction to Modeling High-resolution Spectra, in *Handbook of High Resolution Spectroscopy*, ed.

M. Quack and F. Merkt, Wiley, John Wiley & Sons, Ltd, 2011, vol. 3, ch. 1, pp. 1415–1435.
85 S. Albert, K. Keppler Albert, P. Lerch and M. Quack, *Faraday Discuss.*, 2011, vol. 150, p. 71.
86 S. Albert, K. Keppler Albert and M. Quack, High Resolution Fourier Transform Infrared Spectroscopy, in *Handbook of High Resolution Spectroscopy*, ed. M. Quack and F. Merkt, Wiley, Ltd, 2011, vol. 2, ch. 26, pp. 965–1019.
87 S. Albert, K. Keppler, P. Lerch, M. Quack and A. Wokaun, *J. Mol. Spectrosc.*, 2015, **315**, 92.
88 L. S. Rothman, I. E. Gordon, A. Barbe, D. Chris Benner, P. F. Bernath, M. Birk, V. Boudon, L. R. Brown, A. Campargue, J.-P. Champion, K. Chance, L. H. Coudert, V. Danaj, V. M. Devi, S. Fally, J.-M. Flaud, R. R. Gamache, A. Goldmanm, D. Jacquemart, I. Kleiner, N. Lacome, W. J. Lafferty, J.-Y. Mandin, S. T. Massie, S. N. Mikhailenko, C. E. Miller, N. Moazzen-Ahmadi, O. V. Naumenko, A. V. Nikitin, J. Orphal, V. I. Perevalov, A. Perrin, A. Predoi-Cross, C. P. Rinsland, M. Rotger, M. Šimecková, M. A. H. Smith, K. Sung, S. A. Tashkun, J. Tennyson, R. A. Toth, A. C. Vandaele and J. Vander Auwera, *J. Quant. Spectrosc. Radiat. Transfer*, 2009, **110**, 533.
89 J. K. G. Watson, Aspects of quartic and sextic centrifugal effects on rotational energy levels, in *Vibrational Spectra and Structure*, ed. J. Durig, Elsevier, Amsterdam, 1977, vol. 6, pp. 1–89.
90 A. Bauder, Fundamentals of Rotational Spectroscopy, in *Handbook of High Resolution Spectroscopy*, ed. M. Quack and F. Merkt, Wiley, John Wiley & Sons, Ltd, 2011, vol. 1, ch. 2, pp. 57–116.
91 S. Albert, K. Keppler Albert, H. Hollenstein, C. Manca Tanner and M. Quack, Fundamentals of Rotation-Vibration Spectra, in *Handbok of High Resolution Spectroscopy*, ed. M. Quack and F. Merkt, Wiley & Sons, Chichester, 2011, vol. 2, ch. 3, pp. 117–173.
92 D. Luckhaus and M. Quack, *Mol. Phys.*, 1989, **68**, 745.
93 H. M. Pickett, *J. Mol. Spectrosc.*, 1991, **148**, 371.
94 G. Wichmann, S. Albert, P. Lerch, K. Keppler and M. Quack, *Mol. Phys.*, 2025, e2593929, DOI: **10.1080/00268976.2025.2593929**.
95 M. Quack, *J. Chem. Phys.*, 1985, **82**, 3277.
96 G. Wichmann, G. Seyfang and M. Quack, *Mol. Phys.*, 2021, **119**, e1959073.
97 F. W. Loomis and R. W. Wood, *Phys. Rev.*, 1928, **32**, 223.
98 B. P. Winnewisser, J. Reinstädtler, K. M. T. Yamada and J. Behrend, *J. Mol. Spectrosc.*, 1989, **136**, 12–16.
99 S. Albert, P. Lerch, K. Keppler and M. Quack, THz Spectroscopy of cyano-oxirane ($c$-$C_2H_3OCN$) and methyl oxirane ($c$-$C_2H_3OCH_3$) with synchrotron light, in Proc. 20th Symposium on Atomic, Cluster and Surface Physics 2016 (SASP 2016), Davos, Switzerland, 7 to 12 February 2016'', pp. 165–168, ed. J. Stohner and Ch. Yeretzian, Innsbruck University Press (IUP), Innsbruck, 2016.
100 M. Quack, *Bunsen-Mag.*, 2022, **24**, 238.
101 J. Pochert and M. Quack, *Mol. Phys.*, 1998, **95**, 1055.
102 A. Kushnarenko, V. Krylov, E. Miloglyadov, M. Quack and G. Seyfang, Intramolecular Vibrational Energy Redistribution Measured by Femtosecond Pump–Probe Experiments in a Hollow Waveguide, in ''Ultrafast Phenomena XVI'', Proc. 16th Int. Conf. on Ultrafast Phenomena, Stresa, Italia, June 2008, pages. 349–351 (2009), ed. P. Corkum, S. De Silvestri, K. Nelson, E. Riedle and R. Schoenlein, Springer Series in Chemical Physics, Berlin, 2009.
103 A. Kushnarenko, E. Miloglyadov, M. Quack and G. Seyfang, *Phys. Chem. Chem. Phys.*, 2018, **20**, 10949.
104 R. Marquardt and M. Quack, *Z. Phys. D:At., Mol. Clusters*, 1996, **36**, 229.
105 P. Jakobsen, P. Ferruit, C. Alves de Oliveira, S. Arribas, G. Bagnasco, R. Barho, T. L. Beck, S. Birkmann, T. Böker, A. J. Bunker, S. Charlot, P. de Jong, G. de Marchi, R. Ehrenwinkler, M. Falcolini, R. Fels, M. Franx, D. Franz, M. Funke, G. Giardino, X. Gnata, W. Holota, K. Honnen, P. L. Jensen, M. Jentsch, T. Johnson, D. Jollet, H. Karl, G. Kling, J. Köhler, M.-G. Kolm, N. Kumari, M. E. Lander, R. Lemke, M. López-Caniego, N. Lützgendorf, R. Maiolino, E. Manjavacas, A. Marston, M. Maschmann, R. Maurer, B. Messerschmidt, S. H. Moseley, P. Mosner, D. B. Mott, J. Muzerolle, N. Pirzkal, J.-F. Pittet, A. Plitzke, W. Posselt, B. Rapp, B. J. Rauscher, T. Rawle, H.-W. Rix, A. Rödel, P. Rumler, E. Sabbi, J.-C. Salvignol, T. Schmid, M. Sirianni, C. Smith, P. Strada, M. te Plate, J. Valenti, T. Wettemann, T. Wiehe, M. Wiesmayer, C. J. Willott, R. Wright, P. Zeidler and C. Zincke, *Astron. Astrophys.*, 2022, **661**, A80.
106 P. Ferruit, P. Jakobsen, G. Giardino, T. Rawle, C. Alves de Oliveira, S. Arribas, T. L. Beck, S. Birkmann, T. Böker, A. J. Bunker, S. Charlot, G. de Marchi, M. Franx, A. Henry, D. Karakla, S. A. Kassin, N. Kumari, M. López-Caniego, N. Lützgendorf, R. Maiolino, E. Manjavacas, A. Marston, S. H. Moseley, J. Muzerolle, N. Pirzkal, B. Rauscher, H.-W. Rix, E. Sabbi, M. Sirianni, M. te Plate, J. Valenti, C. J. Willott and P. Zeidler, *Astron. Astrophys.*, 2022, **661**, A81.
107 T. Böker, S. Arribas, N. Lützgendorf, C. Alves de Oliveira, T. L. Beck, S. Birkmann, A. J. Bunker, S. Charlot, G. de Marchi, P. Ferruit, G. Giardino, P. Jakobsen, N. Kumari, M. López-Caniego, R. Maiolino, E. Manjavacas, A. Marston, S. H. Moseley, J. Muzerolle, P. Ogle, N. Pirzkal, B. Rauscher, T. Rawle, H.-W. Rix, E. Sabbi, B. Sargent, M. Sirianni, M. te Plate, J. Valenti, C. J. Willott and P. Zeidler, *Astron. Astrophys.*, 2022, **661**, A82.
108 S. M. Birkmann, P. Ferruit, G. Giardino, L. D. Nielsen, A. García Muñoz, S. Kendrew, B. J. Rauscher, T. L. Beck, C. Keyes, J. A. Valenti, P. Jakobsen, B. Dorner, C. Alves de Oliveira, S. Arribas, T. Böker, A. J. Bunker, S. Charlot, G. de Marchi, N. Kumari, M. López-Caniego, N. Lützgendorf, R. Maiolino, E. Manjavacas, A. Marston, S. H. Moseley, N. Pirzkal, C. Proffitt, T. Rawle, H.-W. Rix, M. te Plate, E. Sabbi, M. Sirianni, C. J. Willott and P. Zeidler, *Astron. Astrophys.*, 2022, **661**, A83.
109 A. Bakasov, T. K. Ha and M. Quack, *J. Chem. Phys.*, 1998, **109**, 7263.

110 B. Fehrensen, D. Luckhaus and M. Quack, *Chem. Phys.*, 2007, **338**, 90.
111 M. Gottselig, D. Luckhaus, M. Quack, J. Stohner and M. Willeke, *Helv. Chim. Acta*, 2001, **84**, 1846.
112 R. Berger, M. Gottselig, M. Quack and M. Willeke, *Angew. Chem.*, 2001, **113**, 4342; R. Berger, M. Gottselig, M. Quack and M. Willeke, *Angew. Chem., Int. Ed.*, 2001, **40**, 4195.
113 H. Hollenstein, D. Luckhaus, J. Pochert, M. Quack and G. Seyfang, *Angew. Chem., Int. Ed. Engl.*, 1997, **36**, 140.
114 R. Berger, M. Quack and J. Stohner, *Angew. Chem., Int. Ed.*, 2001, **40**, 1667.
115 F. Hobi, R. Berger and J. Stohner, *Mol. Phys.*, 2013, **111**, 2345.
116 R. Berger, M. Quack and G. Tschumper, *Helv. Chim. Acta*, 2000, **83**, 1919.
117 M. Quack, Chirality and Molecular Signatures of Life: Detecting and Communicating Life in the Universe, in 15th Brioni Conference on Deep Space Communication, Navigation and Propulsion, Brioni August 2022.
118 M. Guélin and J. Cernicharo, *Front. Astron. Space Sci.*, 2022, **9**, 787567.
119 J. Monod, *Le Hasard et la Nécessité*, Éditions du Seuil, Paris, 1970.
120 S. F. Mason, *Chemical Evolution*, Clarendon Press, Oxford, 1991.
121 M. Eigen, *Steps towards life*, Oxford University Press, Oxford, 1992 (German original: Stufen zum Leben, with Ruthild Winkler-Oswatitsch, translation by Paul Woolley).
122 J. Troe, *Bunsen-Mag.*, 2016, **18**, 228 (lecture on the occasion of receiving the Otto-Hahn-Preis, Paulskirche Frankfurt 24 November 2015).